Accepted Manuscript

Synergistic improvement of epoxy composites with multi-walled carbon nanotubes and hyperbranched polymers

Shuiping Li, Yan Yao

PII: S1359-8368(18)32497-1

DOI: https://doi.org/10.1016/j.compositesb.2018.11.122

Reference: JCOMB 6307

To appear in: *Composites Part B*

Received Date: 7 August 2018

Revised Date: 7 November 2018

Accepted Date: 27 November 2018

Please cite this article as: Li S, Yao Y, Synergistic improvement of epoxy composites with multi-walled carbon nanotubes and hyperbranched polymers, *Composites Part B* (2018), doi: https://doi.org/10.1016/j.compositesb.2018.11.122.

Synergistic Improvement of Epoxy Composites with Multi-walled Carbon Nanotubes and Hyperbranched Polymers

Shuiping Li [a*,b,c], Yan Yao [b]

a School of Materials Science and Engineering, Yancheng Institute of Technology, Yancheng, P. R. China, 224051;

b Institute of Cement Science and New Building Materials, China Building Materials Academy, Beijing, P. R. China, 100024;

c Key Laboratory for Advanced Technology in Environmental Protection of Jiangsu Province, Yancheng Institute of Technology, Yancheng, P. R. China, 224051

Abstract: This paper presented the preparation of composites that consist of multi-walled carbon nanotubes (MWCNTs), hyperbranched polymers (HBPs), epoxy resins (EP) and curing agent. The influences of HBPs and MWCNTs content on the curing process of epoxy systems and mechanical performances of MWCNTs/HBPs/EP composites were discussed. Results from differential scanning calorimeter (DSC), tensile, impact and toughness tests are provided. The tensile and impact fracture surface were observed by field-emission scanning electron microscopy. The addition of HBPs resulted in accelerating the curing process of epoxy systems. MWCNTs/HBPs/EP composites were capable of increasing tensile strength by up to 38 %, giving a tensile modulus of 25 %, impact strength of 68 %, fracture toughness of 66 %, and a glass transition temperature (T_g) of 46 % in comparison with unmodified epoxy thermosets. Field emission-scanning electron micrographs showed that these increases were associated with a synergistic effect of plastic deformation mechanism and crack pinning mechanism, which were induced by the present of HBPs and MWCNTs, respectively.

Keywords: Carbon nanotubes; hyperbranched polymers; epoxy; composites

1 Introduction

Composites have been used extensively in many structure applications owing to their good mechanical properties and improved fatigue life [1-7]. The incorporation of nanoparticles and functional polymers in epoxy composites has been impressive as they significantly improve the properties of epoxy composites [6], especially the tensile strength and fracture toughness [8-11]. In the last decade, carbon nanotubes (CNTs), which exhibit superior mechanical properties, low density, and high aspect ratio, had demonstrated their role as a multi-functional filler for epoxy resins [12-14]. However, the poor dispersity, which is owing to the strong interaction between nanotubes, resulted in the short of expected composite properties [6, 14, 15]. Moreover, the application of CNTs in epoxy composites had been restricted by the lack of sufficient interfacial adhesion [13, 16, 17].

Surface modification of CNTs is a typical approach to enhance the adhesion between CNTs and epoxy matrix [6, 14, 18-20]. Kwon et al. proposed that the difference in mobility of alkyl chains affected the mechanical and impact properties of epoxy resins [16]. Cha and co-workers suggested that the attachment of polystyrene sulfonate and poly(4-aminostyrene) could modify the dispersion and improve affinity with the epoxy matrix [21]. Saeb et al. suggested that the introduction of primary and secondary amino groups could improve the dispersion of MWCNTs and the interfacial interaction in epoxy matrix [22]. Jiang and co-workers proved that the T_gs of CNT/epoxy composites were higher than that of the unmodified epoxy thermosets, which was ascribed to the weak interaction between functionalized CNTs and epoxy matrix [19].

Hyperbranched polymers (HBPs) have been widely used as tougheners for epoxy resins [10, 11,

23-30]. One advantage for the introduction of HBPs to epoxy resins is the high density of terminal functional groups, which can improve affinity with epoxy units and/or curing agents [31]. And a large number of free volumes and free spaces in HBPs are also contributed to the toughness enhancement [32]. Nevertheless, the addition of HBPs to epoxy resins may affect other desirable engineering properties [25].

The purpose of this article was to fabricate MWCNTs/HBPs/EP composites with excellent mechanical properties for potential application in advanced structure materials. The influences of HBPs and MWCNTs content on the curing process of epoxy systems and mechanical properties of MWCNTs/HBPs/EP composites were studied, discussing the results from DSC, tensile, impact, and toughness tests. The novelty of this work is to discuss the synergistic mechanism of HBPs and MWCNTs for enhancing toughness of epoxy composites. The tensile and impact fracture surface of composites were observed using field emission scanning electron microscope (FESEM).

2 Experimental

2.1 Materials

Diglycidyl ether of bisphenol-a resins (EP618), which had an epoxide equivalent of 185-208 g/eq, were obtained from Wuhuigang Adhesive Co., Ltd (Hangzhou, China). Polyamide 650 with an amine value of 220±20 mgKOH/g was purchased from Wuxi Resin Factory (Wuxi, China). Multi-walled carbon nanotubes (MWCNTs), which were specified with average inner and outer diameters of 4 and 12 nm respectively, lengths up to 12 μm, and carbon purity exceeding 95 %, were purchased from Hengqiu Graphene Science & Technology Co., Ltd (Suzhou, China). Diethanolamine was obtained from Tianjin Damao Chemical reagent factory (Tianjin, China). Methyl acrylate and γ-Aminopropyl triethoxysilane were supplied by Sinopharm Chemical

Reagent Co., Ltd (Shanghai, China). Trimethylolpropane was purchased from Tianjin Bodi Chemical Reagent Co., Ltd (Tianjin, China). Oleic acid was obtained from Shanpu Chemical Reagent Co., Ltd (Shanghai, China). Methanol, toluene and H_2O_2 (30 wt%) were supplied by Chengdu Kelong Chemical Reagent Co., Ltd (Chengdu, China). Unless otherwise specified, all chemicals were analytical grade and used as-received. The abbreviations and basic properties of raw materials are listed in Table I.

2.2 Synthesis of HBPs

The synthesis route of HBPs was supposed by Qiang et al. [33]. Typically, 11.6 g of diethanolamine was added to a 250-mL four-necked round-bottom flask with 20 mL of methanol, equipped with a thermometer, inlet and outlet, and condenser tube. 9.55 g of methyl acrylate was added to the flask, heated to 35 ºC and kept under stirring for 4 h. After methanol removed, AB_2 monomers were obtained. 1.34 g of trimethylolpropane was added to 177.63 g of AB_2 monomers, followed by heating to 120 ºC and stirring for 3 h. The crude products were purified under vacuum at 0.08 MPa and 120 ºC for 1 h and then hydroxyl-terminated hyperbranched polymers were obtained. 5 g of oleic acid was added to 10 g of hydroxyl-terminated hyperbranched polymers and then the mixture was heated to 130 ºC and kept under stirring for 2 h. Then the products were dried under vacuum at 80 ºC for 24 h to obtain final HBPs, which contain terminal ester group. All the processes in this study were conducted under a dry nitrogen atmosphere. The synthesis route of HBPs is illustrated in Scheme 1.

2.3 Preparation of MWCNTs/HBPs/EP composites

MWCNTs were first treated with an aqueous solution of H_2O_2 (30 wt%) at 105 ºC for 6 h and then functionalized by γ-Aminopropyl triethoxysilane in toluene at 80 ºC for 24 h. The detailed

modifying procedure was reported in our former work [30]. HBPs and MWCNTs were first stirred at room temperature for 15 min and then added to epoxy resins and polyamide. Epoxy resins, polyamide, HBPs and MWCNTs (Epoxy: polyamide: HBPs: MWCNTs=100: 110: 0-25: 0-2, wt/wt) were blended and homogenized with mechanical stirring at room temperature for 30 min. After removing gas voids under vacuum at 0.09 MPa, the mixture was poured into telflon templates and cured at 60 ºC for 48 h in an oven. The complete preparation process of MWCNTs/HBPs/EP composites is illustrated in Scheme 2.

2.4 Characterization

Differential scanning calorimetry (DSC) was performed with a 200 F3 DSC instrument (NETZSCH, Germany) from -30 to 300 °C at 20 °C min^{-1} under N_2 atmosphere. Tensile testing was performed on dump-bell shaped type samples according to National standard of China (GB/T 2567-2008) with a AG-X plus testing machine (SHIMADZU, Japan) at 2 mm min^{-1}. Charpy impact testing was performed with a ZBC 50 pendulum impact testing machine (SANS, China) without a notch in the specimen with a thickness of 4 mm and a width of 10 mm according to National Standard of China (GB/T 2567-2008). After tensile and impact tests, field emission scanning electron microscope (FESEM) images of fracture surface of composites were recorded by a SU8000 scanning electron microscope (Hitachi, Japan), and the fracture surface were sputter-coated with gold before observation. FESEM micrographs were obtained under conventional secondary electron imaging conditions with an accelerating voltage of 10 kV. Fracture toughness testing was carried out by employing the single-edge-notch beam method on a UTM 4000 universal instrument (SUNS, China) according to National Standard of China (GB/T 4161-2007) at 2 mm min^{-1}. Before testing, a standard-sized notch was milled into the specimen.

And a crack was introduced at the notch-tip by inserting a thin razor blade into the machined notch and pulling with strong force. For each formulation, at least 5 samples were measured to determine the fracture toughness at crack initiation in terms of the critical stress intensity factor, K_{IC} (MPa·m$^{1/2}$). According to the standard used, K_{IC} was calculated using Equation (1):

$$K_{IC} = \frac{PS}{BW^{3/2}} \times \frac{3x^{1/2}[1.99 - x(1-x)(2.15 - 3.93x + 2.7x^2)]}{2(1+2x)(1-x)^{3/2}} \quad (1)$$

Where $x=a/W$ and P is the applied load (N), S is the span (mm), B and W are the specimen thickness and width respectively (mm, mm), and a is the length of crack (mm).

3 Results and discussion

3.1 Curing thermal parameters

The effects of HBPs content on the curing thermal parameters of epoxy systems were summarized in Table II and presented in Figure 1. It can be observed that the curing process of epoxy systems is rather simple, with a single exothermic peak in the range of 50-250 °C. The onset temperature (T_o), exothermic peak temperature (T_p), ending temperature (T_E), and enthalpy of reaction (Δh) are also determined. Table II and Figure 1 show that the T_o, T_p and T_E of HBPs modified epoxy systems are all shifted to lower temperatures with increment of HBPs content, comparing with unmodified system, which were due to the enhanced reactive rate in the present of HBPs. The stoichiometric rate of amino group to epoxide group had been changed because of the volatilization of amino group in whole curing process [23]. Then the reactive rates of HBPs modified epoxy systems are higher than unmodified system, which can be attributed to the supplementary of functional groups. Moreover, the curing rate of HBPs modified epoxy systems can also be promoted owing to the nucleophilic attack of carboxyl in HBPs to an epoxy unit in epoxy matrix [34] and the interaction of ester in HBPs and epoxide in matrix [28].

3.2 Mechanical properties

Mechanical properties of HBPs modified epoxy thermosets are summarized in Table III. A conclusion can be drawn that the mechanical properties are highly dependent on HBPs content. In details, tensile strength, tensile modulus, elongation at break, and impact strength are obviously higher than those of unmodified epoxy thermosets. Especially, the formulation with 20 wt% HBPs yields the tensile strength, tensile modulus, elongation at break, and impact strength of 48.7 MPa, 1.42 GPa, 6.0 % and 12.24 KJ/m^2, which had an increase of 38.4 %, 25.4 %, 71.2 % and 68.4 %, respectively, comparing with unmodified epoxy system. These results demonstrate that the introduction of HBPs to epoxy thermosets can contribute to the improvement of mechanical properties. The carboxyl and ester functional groups in HBPs, forming hydrogen bond [32] and covalent bond [35, 36] with epoxide groups, can also promote the interfacial adhesion between HBPs and epoxy matrix [36]. However, the improvement of mechanical properties is short of expectation owing to the flexible chains in HBPs.

The fracture toughness of HBPs modified epoxy thermosets increases with increasing HBPs content and is higher than that of unmodified epoxy thermosets (Table III). Especially, the fracture toughness of formulation with 20 wt% HBPs is 1.90 $MPa \cdot m^{1/2}$, which had an increase of 35.7 % in comparison with unmodified epoxy thermosets. HBPs possess high density terminal functional groups, which can react with epoxide groups in epoxy matrix and/or amino groups in curing agent and consequently, the network of epoxy thermosets can be tailored [31, 32]. The free volumes and free spaces in network can be increased owing to the introduction of HBPs [32]. The decrease of toughness of 25 wt% HBPs modified epoxy thermosets may be due to the formation of HBPs continuous phase in epoxy thermosets, which exhibits a low fracture resistance as a separate

phase.

Mechanical properties of MWCNTs/HBPs/EP composites are summarized in Table IV. The mechanical properties of composites are highly dependent on MWCNTs content and higher than those of 20 wt% HBPs modified and also unmodified epoxy thermosets. The sample with 1.0 wt% MWCNTs exhibits tensile strength, tensile modulus, elongation at break, and impact strength of 57.8 MPa, 1.83 GPa, 8.3 %, and 16.8 KJ/m^2, which had an increase of 64.2 %, 66.4 %, 137.1 % and 130.1 %, respectively, comparing with unmodified epoxy thermosets. The hydroxyl and amino groups of MWCNTs, which can interact with functional groups of epoxy units in the presence of HBPs, can be attributed to the significant improvement of interfacial adhesion between MCWNTs and epoxy matrix [36] and consequently, enhance the mechanical properties of composites. Moreover, MWCNTs can pin or blunt the crack propagation due to their tiny sizes, then absorb external loading energy and result in the stabilization of cracks in epoxy matrix [10, 15, 37]. Furthermore, external loading may transfer from epoxy matrix to MWCNTs, thus MWCNTs may stretch and break, which can also lead to the increase of mechanical properties of composites [15].

Table IV indicates that the fracture toughness of MWCNTs/HBPs/EP composites is higher than those of 20 wt% HBPs modified and unmodified epoxy thermosets. And the toughness of MWCNTs/HBPs/EP composites increases with the increment of MWCNTs content. In particular, the fracture toughness of composites with 1.0 wt% MWCNTs is 2.32 MPa·$m^{1/2}$, which shows an increase of 65.7 % and 22.1 % in comparison with unmodified and 20 wt% HBPs modified epoxy thermosets, respectively. These results reveal that the enhancement of fracture toughness can be attributed to the addition of MWCNTs, which can contribute to improve the interfacial failure

resistance of epoxy matrix [38]. Moreover, the addition of MWCNTs in epoxy composites may contribute to shear inducing deformation, consuming external energy and crack deflection. Especially, MWCNTs may act as “pin” when the crack propagation passes through them [38].

3.3 Glass transition temperature

Table V lists glass transition temperatures (T_gs) of HBPs modified epoxy thermosets. Unmodified epoxy system presents a T_g of 118.9 ºC and is lower than those of HBPs modified epoxy thermosets. Especially, 20 wt% HBPs modified sample presents a T_g of 164.3 ºC, presenting an increase of 45.4 ºC in comparison with unmodified epoxy thermosets. Furthermore, the T_g of HBPs modified epoxy thermosets increases with increasing HBPs content, which indicates an increase of crosslinking density in epoxy matrix [39]. The functional carboxyl and ester groups in HBPs, which can implement a nucleophilic attack [34] and interact to/with epoxide group, respectively, cannot only promote the curing rate of epoxy systems but also improve the crosslinking density of epoxy thermosets, resulting in restricting the motion of molecular fragment [27]. However, the T_g of 20 wt% HBPs modified epoxy thermosets decreases, which may be attributed to that HBPs content was higher than a certain threshold value and resulting in a poor disperse in epoxy matrix [23].

The T_gs of MWCNTs/HBP/EP composites are listed in Table VI. It can be seen that the T_gs of MWCNTs/HBP/EP composites are higher than those of unmodified and HBPs modified epoxy thermosets. In detail, composites with 20 wt% HBPs and 1 wt% MWCNTs exhibits a T_g of 173.2 ºC, which had an increase of 46 % and 5 % in comparison with unmodified and 20 wt% HBPs modified epoxy thermosets, respectively. Moreover, T_g of composites increases with increasing MWCNTs content. The MWCNTs were well dispersion in MWCNTs/HBP/EP composites, which

was owing to excellent interaction of MWCNTs and epoxy matrix in the present of HBPs, and then restricted the motion of molecular segment.

3.4 SEM morphologies

The improved mechanical properties of HBPs modified epoxy thermosets and composites were also evidenced by observing the morphologies of their fracture surface using FESEM. The FESEM images of tensile fracture surface of HBPs modified epoxy thermosets and composites are shown in Figure 2. The FESEM image of tensile fracture surface of unmodified epoxy thermosets shows no dimple that indicates a brittle fracture (Figure 2a). The morphology of tensile fracture surface of 20 wt% HBPs modified epoxy thermosets (Figure 2b) shows a large number of dimples, which can be attributed to good flexibility of HBPs and excellent compatibility of HBPs and epoxy matrix. Actually, FESEM image of HBPs modified epoxy thermosets shows more plastic deformations than that of unmodified epoxy thermosets. However, the morphology of tensile fracture surface of composites with 1.0 wt% MWCNTs only presents several dimples owing to weak dispersion of MWCNTs in epoxy systems (Figure 2c). The tensile fracture surface of composites with 20 wt% HBPs and 1.0 wt% MWCNTs exhibits an obvious dimple (Figure 2d). These results indicate that the introduction of HBPs can improve the plastic deformation of epoxy thermosets and composites, which is due to the functional terminal groups and flexible chains in HBPs. And the addition of MWCNTs may restrict the crack propagation and result in a relatively large dimple.

Figure 3 shows FESEM images of impact fracture surface of HBPs modified epoxy thermosets and composites. The image of unmodified epoxy thermosets shows a smooth impact fracture surface (Figure 3a), which is a typical brittle fracture morphology of polymers [15]. The impact

surface of HBPs modified epoxy thermosets (Figure 3b), which presents several multi-scale deformations, is much rougher than that of unmodified epoxy thermosets. This difference demonstrates that the introduction of HBPs in epoxy thermosets may result in plastic deformation. MWCNTs can be observed in the fracture surface of epoxy composites with 1.0 wt% MWCNTs (Figure 3c). However, the dispersion of MWCNTs in epoxy systems is not so “satisfactory”. In the fracture impact surface of composites with 20 wt% HBPs and 1.0 wt% MWCNTs (Figure 3d), several deformation and aggregated MWCNTs in the front of crack-pin can be observed. The EDS spectrum of a selected area in composites with 20 wt% HBPs and 1.0 wt% MWCNTs, which was marked in red, is shown in Figure 3e. This spectrum is simple and, presents three elements, C, O and Si. It can be realized that the spectrum of epoxy matrix should contain N element, which is attributed to the use of curing agent, polyamide 650. However, there was no signal peak of N element in this EDS spectrum. Moreover, Si element signal, which is original from silanized MWCNTs, appeared. There results indicate that the selected area was main consisted of MWCNTs.

It can be concluded that the incorporation of MWCNTs in epoxy systems may lead to crack pinning effect and then adsorb external energy. All in all, the fracture impact surface of modified thermosets and composites are much rougher than that of unmodified epoxy thermosets. The fracture surface of composites presents crack-pinning or crack-blunting and also evident deformation. The deformation is likely associated with the excellent functional terminal groups in HBPs, which can interact with epoxide group and result in the formation of free volumes and free spaces. The crack-pinning or crack-blunting effect may be attributed to well dispersion of MWCNTs [16], which leads to crack propagations, crack deflections and crack pins.

Figure 4 is the magnified images of aggregated MWCNTs in composites. Figure 4a, which shows the magnified image of aggregated MWCNTs in composites with 1.0 wt% MWCNTs, exhibits that MWCNTs are “well dispersive’ in the surface. The magnified image of aggregated MWCNTs in composites with 20 wt% HBPs and 1.0 wt% MWCNTs (Figure 4b) shows good dispersive than that of composites with 1.0 wt% MWCNTs, which may be attributed to the present of HBPs. And the distribution density of MWCNTs in Figure 4a is higher than in Figure 4b. This result suggests that the introduction of HBPs in composites with MWCNTs may result in an improving dispersion of MWCNTs.

The toughness mechanisms of epoxy composites, consisting of MWCNTs and HBPs can be concluded as follows: the presents of HBPs can result in the formation of plastic deformation owing to their good flexibility of HBPs and excellent compatibility of HBPs and epoxy systems. The deformation can absorb loading energy and result in the improvement of toughness and other mechanical properties. Moreover, the addition of HBPs can “improve” the dispersion of MWCNTs in epoxy composites. MWCNTs can pin in the front of cracks and result in crack-blunting, crack-pinning, propagation and crack deflection, and the toughness of epoxy composites is certainly improved. So the toughness mechanisms of composites, consisting of MWCNTs and HBPs, can be attributed to the synergistic mechanism of plastic deformation mechanism and crack pinning mechanism, which are induced by HBPs and MWCNTs, respectively.

4 Conclusions

Hyperbranched polymers (HBPs), which contain terminal ester group, were synthesized by using oleic acid modifying hydroxyl-terminated HBPs. Epoxy composites, consisting of

multi-walled carbon nanotubes (MWCNTs), HBPs, epoxy resins (EP) and curing agent, were prepared. The influence of HBPs on the curing process of epoxy systems was studied. And the mechanical properties of MWCNTs/HBPs/EP composites were investigated, resulting from tensile, impact and toughness tests. The introduction of HBPs could result in the improvement of reactive rate and accelerating curing process of epoxy systems. And composites containing 20 wt% HBPs and 1.0 wt% MWCNTs presented excellent mechanical performances. The microstructure morphology analyses of fracture surface indicated that the toughening mechanisms could be attributed to the synergistic mechanisms of plastic deformation mechanism and crack pinning mechanism, which were attributed to HBPs and MWCNTs, respectively.

Acknowledgements

This study was funded by the National Natural Science Foundation of China (51603179 and 51502259), the Six Talent Peaks Project in Jiangsu Province (2017-GDZB-053 and 2016-XCL-070), the joint research fund between Collaborative Innovation Center for Ecological Building Materials and Environmental Protection Equipments of Jiangsu province, the joint research fund between Collaborative Innovation Center for Ecological Building Materials (CP201506), and the Top-notch Academic Programs Project of Jiangsu Higher Education Institutions (PPZY2015A025).

Notes The authors declare that they have no conflict of interest.

Dr. Shuiping Li is a visiting scholar at China Building Materials Academy.

References

1. N. Tual, N. Carrere, P. Davies, T. Bonnemains, and E. Lolive, *Characterization of sea water ageing effects on mechanical properties of carbon/epoxy composites for tidal*

turbine blades. Composites Part A: Applied Science and Manufacturing, 2015. **78**: p. 380-389.

2. A. Tutunchi, R. Kamali, and A. Kianvash, *Effect of Al2O3nanoparticles on the steel-glass/epoxy composite joint bonded by a two-component structural acrylic adhesive.* Soft Materials, 2016. **14**(1): p. 1-8.

3. M.S. Lee, S.J. Kim, O.D. Lim, and C.G. Kang, *The effect process parameters on epoxy flow behavior and formability with CR340/CFRP composites by different laminating in deep drawing process.* Journal of Materials Processing Technology, 2016. **229**: p. 275-285.

4. P. Silva, P. Fernandes, J. Sena-Cruz, J. Xavier, F. Castro, D. Soares, and V. Carneiro, *Effects of different environmental conditions on the mechanical characteristics of a structural epoxy.* Composites Part B: Engineering, 2016. **88**: p. 55-63.

5. H. Zhou, X. Du, H.-Y. Liu, H. Zhou, Y. Zhang, and Y.-W. Mai, *Delamination toughening of carbon fiber/epoxy laminates by hierarchical carbon nanotube-short carbon fiber interleaves.* Composites Science and Technology, 2017. **140**: p. 46-53.

6. M.R. Zakaria, H.M. Akil, M.H.A. Kudus, and S.S.M. Saleh, *Enhancement of tensile and thermal properties of epoxy nanocomposites through chemical hybridization of carbon nanotubes and alumina.* Composites Part A: Applied Science and Manufacturing, 2014. **66**: p. 109-116.

7. C. Jiang, K. Fan, F. Wu, and D. Chen, *Experimental study on the mechanical properties and microstructure of chopped basalt fibre reinforced concrete.* Materials and Design, 2014. **58**: p. 187-193.

8. R.K. Prusty, D.K. Rathore, and B.C. Ray, *Evaluation of the role of functionalized CNT in glass fiber/epoxy composite at above- and sub-zero temperatures: Emphasizing interfacial microstructures.* Composites Part A: Applied Science and Manufacturing, 2017. **101**: p. 215-226.

9. A. Kumar, P.K. Ghosh, K.L. Yadav, and K. Kumar, *Thermo-mechanical and anti-corrosive properties of MWCNT/epoxy nanocomposite fabricated by innovative dispersion technique.* Composites Part B: Engineering, 2017. **113**: p. 291-299.

10. J.M. Misasi, Q. Jin, K.M. Knauer, S.E. Morgan, and J.S. Wiggins, *Hybrid POSS-Hyperbranched polymer additives for simultaneous reinforcement and toughness improvements in epoxy networks.* Polymer, 2017. **117**: p. 54-63.

11. X. Fei, W. Wei, Y. Tang, Y. Zhu, J. Luo, M. Chen, and X. Liu, *Simultaneous enhancements in toughness, tensile strength, and thermal properties of epoxy-anhydride thermosets with a carboxyl-terminated hyperbranched polyester.* European Polymer Journal, 2017. **90**: p. 431-441.

12. D. Micheli, A. Vricella, R. Pastore, A. Delfini, A. Giusti, M. Albano, M. Marchetti, F. Moglie, and V.M. Primiani, *Ballistic and electromagnetic shielding behaviour of multifunctional Kevlar fiber reinforced epoxy composites modified by carbon nanotubes.* Carbon, 2016. **104**: p. 141-156.

13. Y. Li and X. Huang, *Dispersion evaluation, processing and tensile properties of carbon nanotubes-modified epoxy composites prepared by high pressure homogenization.* Composites Part A: Applied Science and Manufacturing, 2015. **78**: p. 166-173.

14. W. Yu, J. Fu, L. Chen, P. Zong, J. Yin, D. Shang, Q. Lu, H. Chen, and L. Shi, *Enhanced*

thermal conductive property of epoxy composites by low mass fraction of organic–inorganic multilayer covalently grafted carbon nanotubes. Composites Science and Technology, 2016. **125**: p. 90-99.

15. Q. Guan, L. Yuan, Y. Zhang, A. Gu, and G. Liang, *Improving the mechanical, thermal, dielectric and flame retardancy properties of cyanate ester with the encapsulated epoxy resin-penetrated aligned carbon nanotube bundle.* Composites Part B: Engineering, 2017. **123**: p. 81-91.
16. D.-J. Kwon, Z.-J. Wang, J.-Y. Choi, P.-S. Shin, K.L. DeVries, and J.-M. Park, *Interfacial and mechanical properties of epoxy composites containing carbon nanotubes grafted with alkyl chains of different length.* Composites Part A: Applied Science and Manufacturing, 2016. **82**: p. 190-197.
17. A.P. Kharitonov, A.G. Tkachev, A.N. Blohin, T.P. Dyachkova, D.E. Kobzev, A.V. Maksimkin, A.S. Mostovoy, and L.N. Alekseiko, *Reinforcement of Bisphenol-F epoxy resin composites with fluorinated carbon nanotubes.* Composites Science and Technology, 2016. **134**: p. 161-167.
18. M.E. Shabestari, E.N. Kalali, V.J. González, D.-Y. Wang, J.P. Fernández-Blázquez, J. Baselga, and O. Martin, *Effect of nitrogen and oxygen doped carbon nanotubes on flammability of epoxy nanocomposites.* Carbon, 2017. **121**: p. 193-200.
19. C. Jiang, J. Zhang, S. Lin, S. Ju, and D. Jiang, *Effects of free organic groups in carbon nanotubes on glass transition temperature of epoxy matrix composites.* Composites Science and Technology, 2015. **118**: p. 269-275.
20. R. Wang, H. Wang, L. Sun, E. Wang, Y. Zhu, and Y. Zhu, *The fabrication and tribological*

behavior of epoxy composites modified by the three-dimensional polyurethane sponge reinforced with dopamine functionalized carbon nanotubes. Applied Surface Science, 2016. **360, Part A**: p. 37-44.

21. J. Cha, S. Jin, J.H. Shim, C.S. Park, H.J. Ryu, and S.H. Hong, *Functionalization of carbon nanotubes for fabrication of CNT/epoxy nanocomposites.* Materials & Design, 2016. **95**: p. 1-8.

22. M.R. Saeb, F. Najafi, E. Bakhshandeh, H.A. Khonakdar, M. Mostafaiyan, F. Simon, C. Scheffler, and E. Mäder, *Highly curable epoxy/MWCNTs nanocomposites: An effective approach to functionalization of carbon nanotubes.* Chemical Engineering Journal, 2015. **259**: p. 117-125.

23. S. Li, Q. Wu, T. Lv, H. Zhu, H. Hou, Q. Lin, Y. Li, C. Cui, and Y. Guo, *Synthesis and characterization of hyperbranched polymer with epoxide-terminated group and application as modifier for epoxy/polyamide system.* Polymer Science, Series B, 2017. **59**(3): p. 328-336.

24. S. Li, Q. Wu, C. Cui, H. Zhu, H. Hou, Q. Lin, Y. Li, and T. Lv, *Synergetic reinforcements of epoxy composites with glass fibers and hyperbranched polymers.* Polymer Composites, 2017. **39**(8): p. 2871-2879.

25. Z.-P. Zou, X.-B. Liu, Y.-P. Wu, B. Tang, M. Chen, and X.-L. Zhao, *Hyperbranched polyurethane as a highly efficient toughener in epoxy thermosets with reaction-induced microphase separation.* RSC Advances, 2016. **6**(22): p. 18060-18070.

26. F. Shiravand, L. Ascione, P. Persico, C. Carfagna, T. Brocks, M.O.H. Cioffi, C. Puglisi, F. Samperi, and V. Ambrogi, *A novel hybrid linear-hyperbranched poly(butylene adipate)*

copolymer as an epoxy resin modifier with toughening effect. Polymer International, 2016. **65**(3): p. 308-319.

27. S. Li, H. Zhu, T. Lv, Q. Lin, H. Hou, Y. Li, Q. Wu, and C. Cui, *The effect of amino-terminated hyperbranched polymers on the impact resistance of epoxy resins.* Colloid and Polymer Science, 2016. **294**(3): p. 607-615.

28. L. Pan, S. Lu, X. Xiao, Z. He, C. Zeng, J. Gao, and J. Yu, *Enhanced mechanical and thermal properties of epoxy with hyperbranched polyester grafted perylene diimide.* Rsc Advances, 2015. **5**(5): p. 3177-3186.

29. S. Li, C. Cui, and H. Hou, *Synthesis and characterization of amino-terminated hyperbranched polymer and as modifier for epoxy resin thermosets.* Colloid and Polymer Science, 2015. **293**(9): p. 2681-2688.

30. S. Li, C. Cui, H. Hou, Q. Wu, and S. Zhang, *The effect of hyperbranched polyester and zirconium slag nanoparticles on the impact resistance of epoxy resin thermosets.* Composites Part B: Engineering, 2015. **79**: p. 342-350.

31. D. Ratna and G.P. Simon, *Thermomechanical properties and morphology of blends of a hydroxy-functionalized hyperbranched polymer and epoxy resin.* Polymer, 2001. **42**(21): p. 8833-8839.

32. J.-P. Yang, Z.-K. Chen, G. Yang, S.-Y. Fu, and L. Ye, *Simultaneous improvements in the cryogenic tensile strength, ductility and impact strength of epoxy resins by a hyperbranched polymer.* Polymer, 2008. **49**(13–14): p. 3168-3175.

33. T.T. Qiang, Q.Q. Bu, Z.F. Huang, and X.C. Wang, *Synthesis and Characterization of Hyperbranched Linear Surfactants.* Journal of Surfactants and Detergents, 2014. **17**(2): p.

215-221.

34. X. Fernández-Francos, A. Rybak, R. Sekula, X. Ramis, and A. Serra, *Modification of epoxy–anhydride thermosets using a hyperbranched poly(ester-amide): I. Kinetic study.* Polymer International, 2012. **61**(12): p. 1710-1725.

35. M. Li, Y. Gu, Y. Liu, Y. Li, and Z. Zhang, *Interfacial improvement of carbon fiber/epoxy composites using a simple process for depositing commercially functionalized carbon nanotubes on the fibers.* Carbon, 2013. **52**: p. 109-121.

36. X. Sui, J. Shi, H. Yao, Z. Xu, L. Chen, X. Li, M. Ma, L. Kuang, H. Fu, and H. Deng, *Interfacial and fatigue-resistant synergetic enhancement of carbon fiber/epoxy hierarchical composites via an electrophoresis deposited carbon nanotube-toughened transition layer.* Composites Part a-Applied Science and Manufacturing, 2017. **92**: p. 134-144.

37. C. Ma, S. Qiu, B. Yu, J. Wang, C. Wang, W. Zeng, and Y. Hu, *Economical and environment-friendly synthesis of a novel hyperbranched poly(aminomethylphosphine oxide-amine) as co-curing agent for simultaneous improvement of fire safety, glass transition temperature and toughness of epoxy resins.* Chemical Engineering Journal, 2017. **322**: p. 618-631.

38. N. Zheng, Y. Huang, H.-Y. Liu, J. Gao, and Y.-W. Mai, *Improvement of interlaminar fracture toughness in carbon fiber/epoxy composites with carbon nanotubes/polysulfone interleaves.* Composites Science and Technology, 2017. **140**: p. 8-15.

39. T. Liu, Y. Nie, L. Zhang, R. Chen, Y. Meng, and X. Li, *Dependence of epoxy toughness on the backbone structure of hyperbranched polyether modifiers.* Rsc Advances, 2015. **5**(5):

p. 3408-3416.

Table I Abbreviations and basic properties of raw materials

Reagent	abbreviation	basic propertie	Supplier
Epoxy resin	EP	epoxide equivalent: 185-208 g/eq	Wuhuigang Adhesive
Polyamide 650	PA	amine value: 220±20 mgKOH/g	Wuxi Resin Factory
Multi-walled carbon nanotubes	MWCNTs	inner and outer diameters: 4 and 12 nm; lengths: ~12 μm; carbon purity: > 95 %	Hengqiu Graphene Science & Technology
Diethanolamine	DA	analytical grade	Tianjin Damao Chemical reagent factory
Methyl acrylate	MA	analytical grade	Sinopharm Chemical Reagent
γ-Aminopropyl triethoxysilane	γ-APS	analytical grade	
Oleic acid	OA	analytical grade	Shanpu Chemical Reagent
Methanol		analytical grade	Chengdu Kelong Chemical Reagent
H_2O_2		30 wt%	
toluene		analytical grade	

Table II The thermal parameters of the uncured epoxy systems with HBPs

Content, wt%	T_o, ºC	T_p, ºC	T_E, ºC	Δh (J g^{-1})
unmodified	86.2	136.3	179.4	226.8
10	83.0	129.3	184.4	368.3
15	82.2	128.6	174.8	710.3
20	66.7	127.3	170.4	621.7
25	80.5	124.4	179.6	961.0

T_o, T_p, T_E, and Δh denote the onset temperature, exothermic peak temperature, ending temperature, and enthalpy of reaction, respectively.

Table III Mechanical and fracture toughness of HBPs modified epoxy thermosets

Content (wt%)	Tensile strength (MPa)	Tensile modulus (GPa)	Elongation (%)	Impact strength (KJ/m^2)	Fracture toughness ($MPa \cdot m^{1/2}$)
unmodified	35.2±1.9	1.06±0.08	3.5±0.26	7.27±0.32	1.40±0.11
10	42.8±1.8	1.43±0.09	4.7±0.33	8.95±0.45	1.53±0.17
15	46.8±2.3	1.61±0.06	5.8±0.28	10.99±0.21	1.75±0.20
20	48.7±1.2	1.65±0.07	6.0±0.22	12.24±0.28	1.90±0.18
25	46.3±1.9	1.59±0.07	5.6±0.19	12.21±0.42	1.74±0.13

Table IV Mechanical and fracture toughness of MWCNTs/HBPs/epoxy composites

MWCNTs (wt%)	Tensile strength (MPa)	Tensile modulus (GPa)	Elongation (%)	Impact strength (KJ/m^2)	Fracture toughness ($MPa \cdot m^{1/2}$)
20wt% HBPs modified	48.7±3.1	1.65±0.07	6.0±0.34	12.22±0.29	1.90±0.20
0.5	51.5±2.7	1.72±0.05	7.5±0.42	13.84±0.35	2.19±0.19
1.0	57.8±1.9	1.83±0.05	8.3±0.29	16.87±0.27	2.32±0.20
1.5	55.4±2.4	1.79±0.06	8.0±0.18	15.72±0.31	2.16±0.18
2.0	53.9±2.0	1.72±0.05	7.8±0.27	15.35±0.30	2.10±0.21

Table V T_gs of HBP modified epoxy thermosets

	unmodified	HBP content (wt%)			
		10	15	20	25
T_gs(ºC)	118.9±1.5	137.8±2.7	151.3±2.2	164.3±3.0	154.7±3.2

Table VI T_gs of MWCNTs/HBPs/epoxy composites

	unmodified	20 wt% HBP modified	MWCNTs content (wt%)			
			0.5	1.0	1.5	2.0
T_gs(ºC)	118.9±1.5	164.3±2.6	168.8±3.0	173.2±3.5	174.7±2.3	175.8±2.9

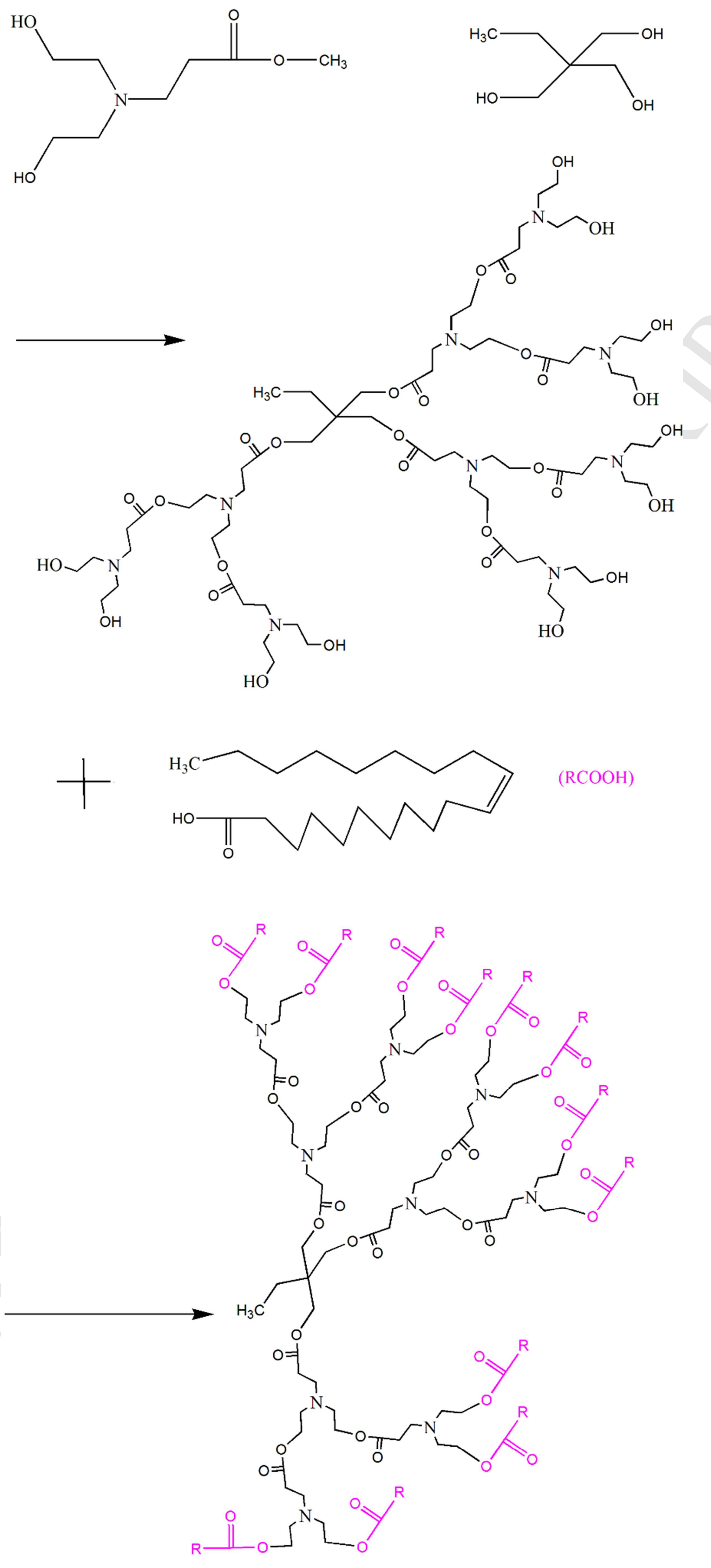

Scheme 1 The synthesis route of HBPs

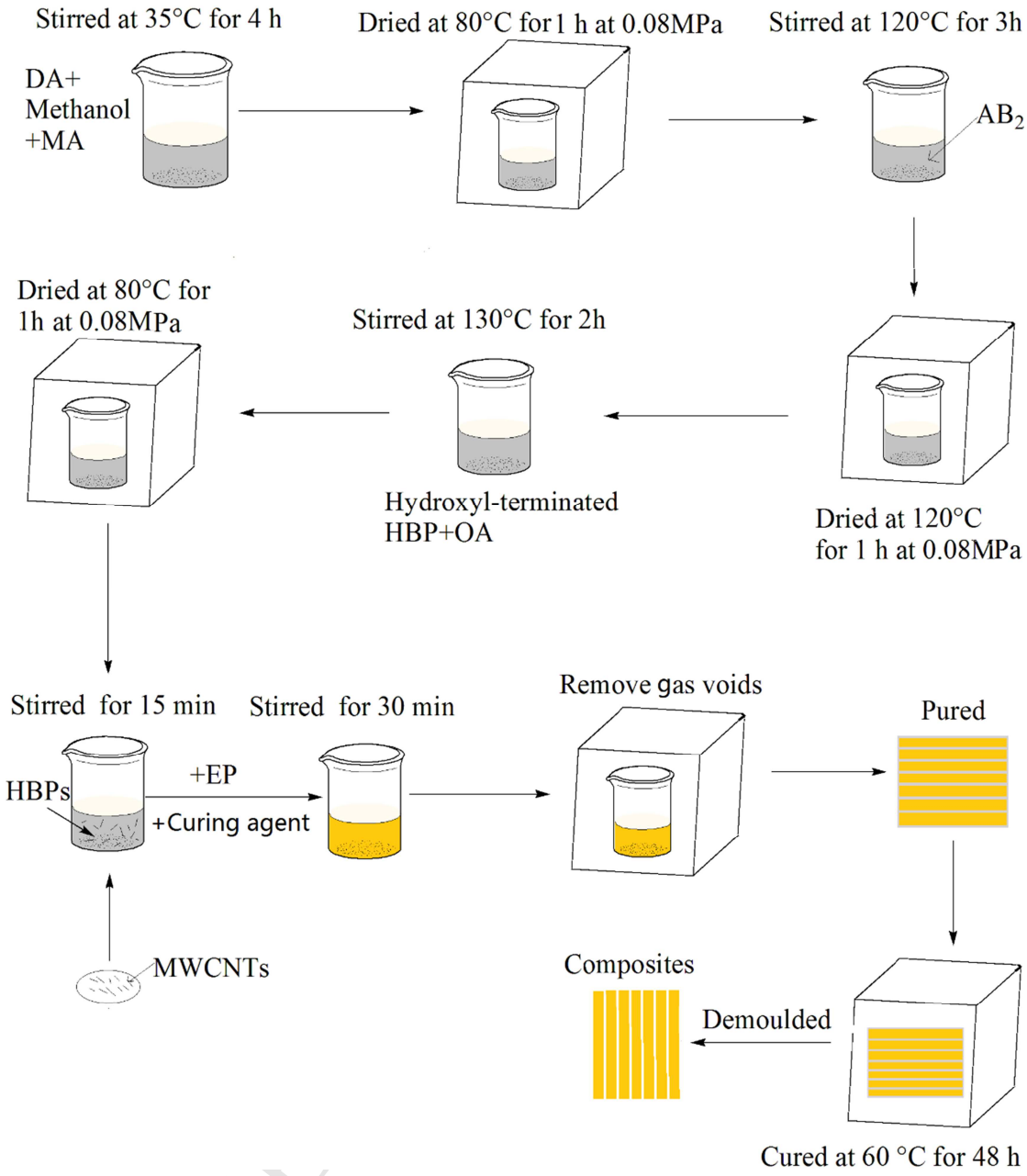

Scheme 2 Detailed preparation process of MWCNTs/HBPs/EP composites

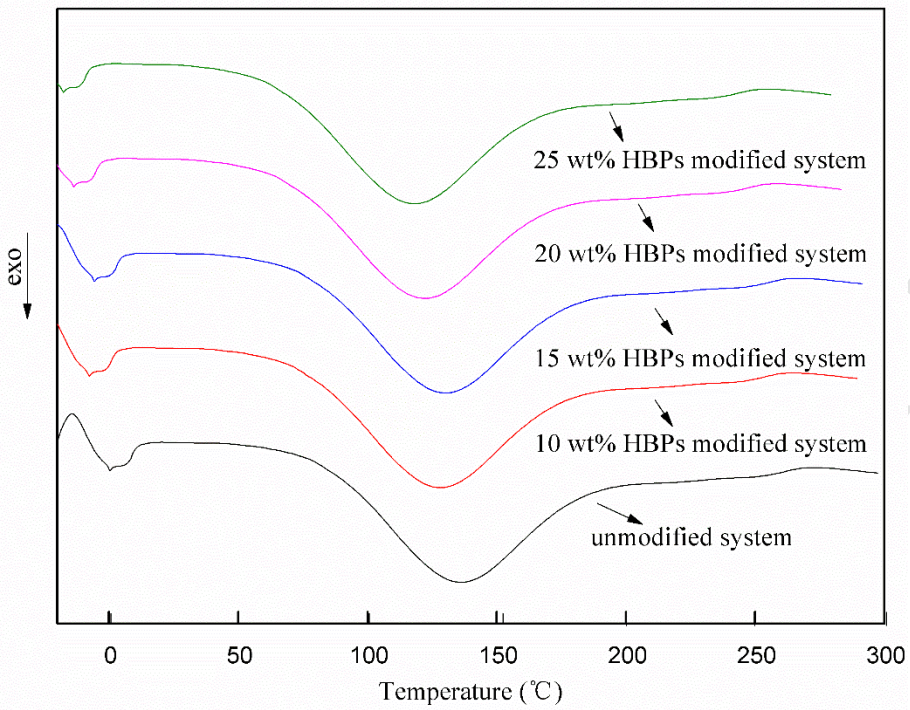

Figure 1 DSC curves of the uncured epoxy systems with HBPs

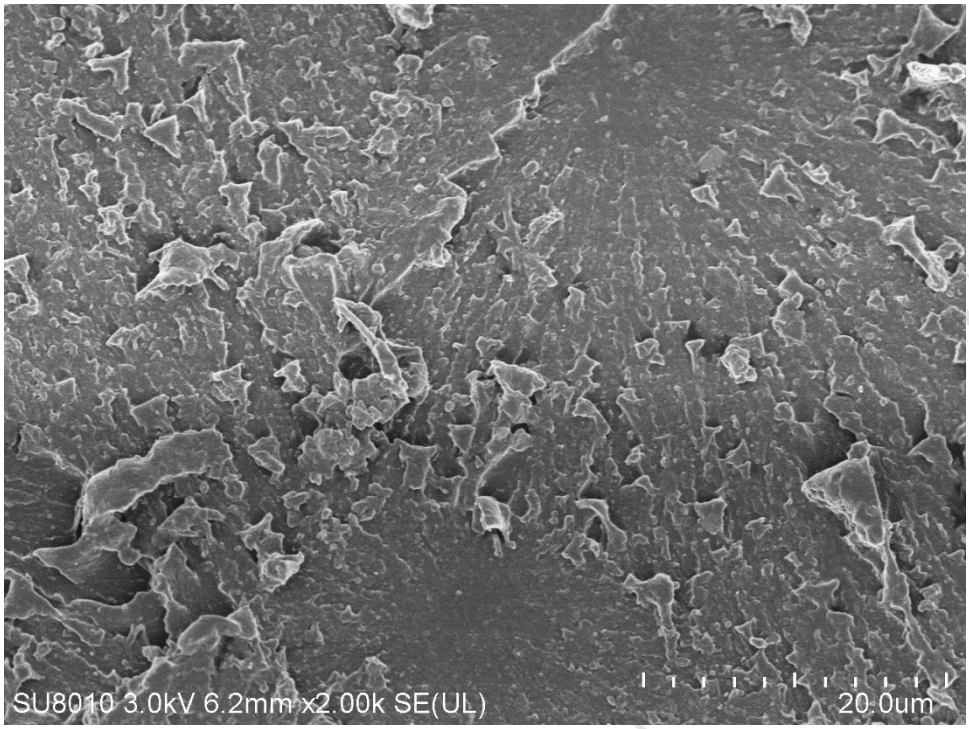

Figure 2a SEM image of the tensile fracture surface of the unmodified thermosets

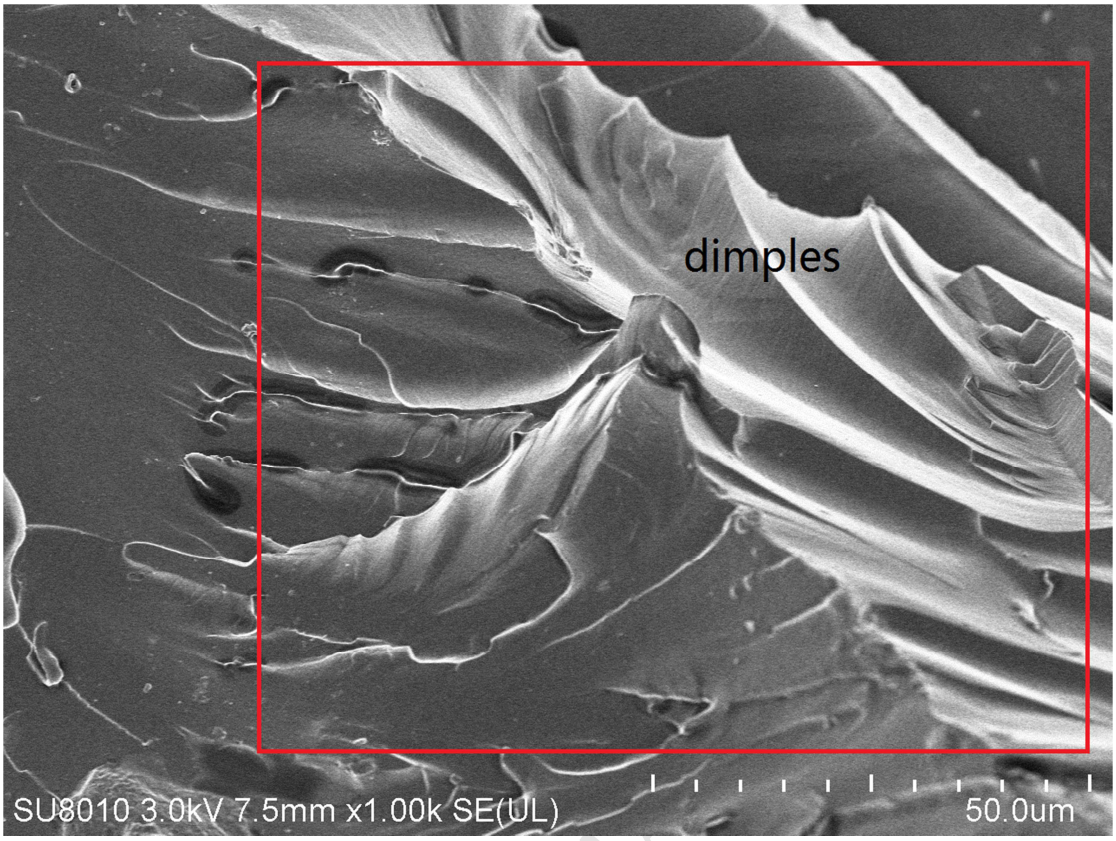

Figure 2b SEM image of the tensile fracture surface of the 20 wt% HBPs modified thermosets

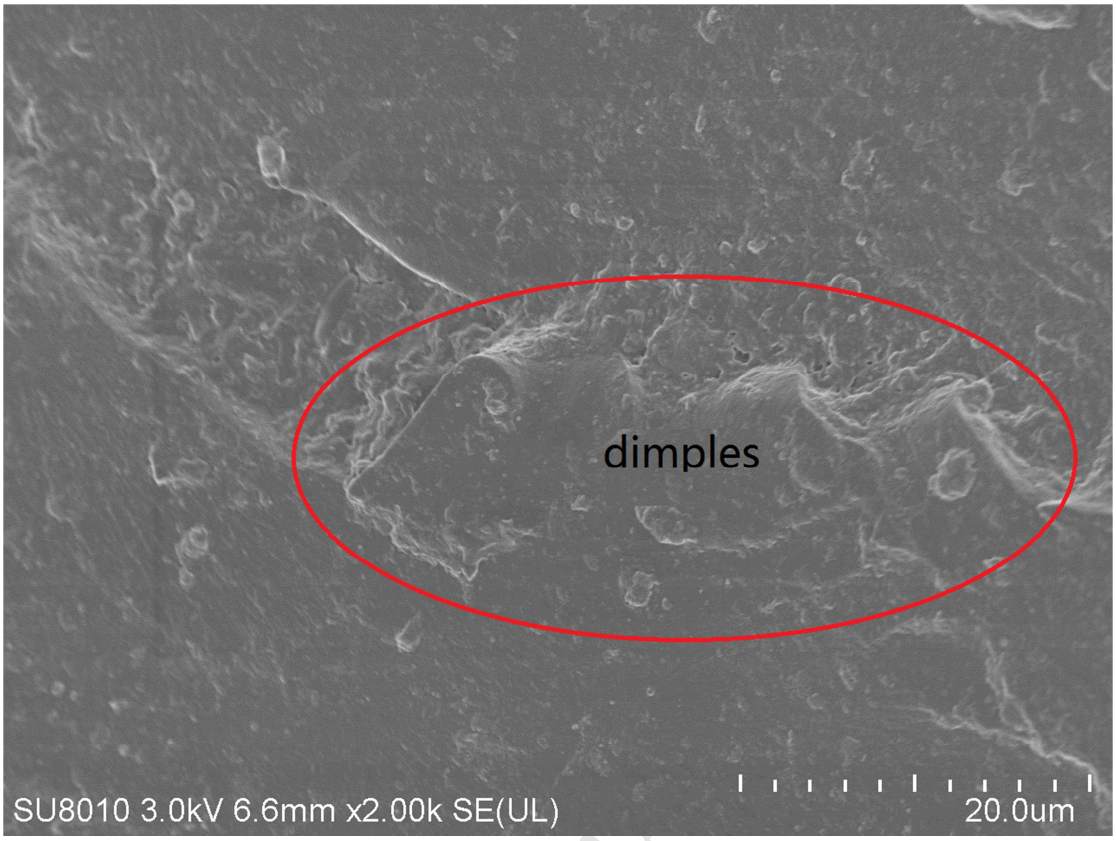

Figure 2c SEM image of the tensile fracture surface of the composites with 1.0 wt% MWCNTs

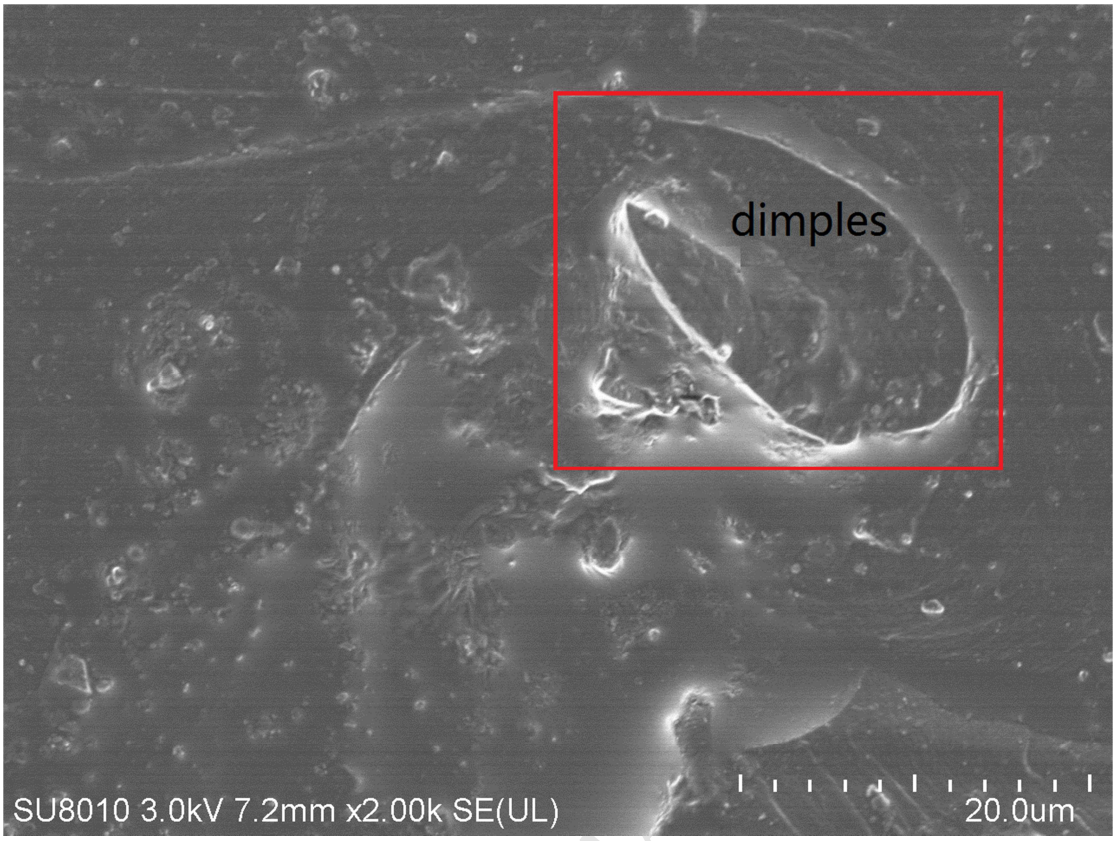

Figure 2d SEM image the tensile fracture surface of the composites with 20 wt% HBPs and 1 wt% MWCNTs

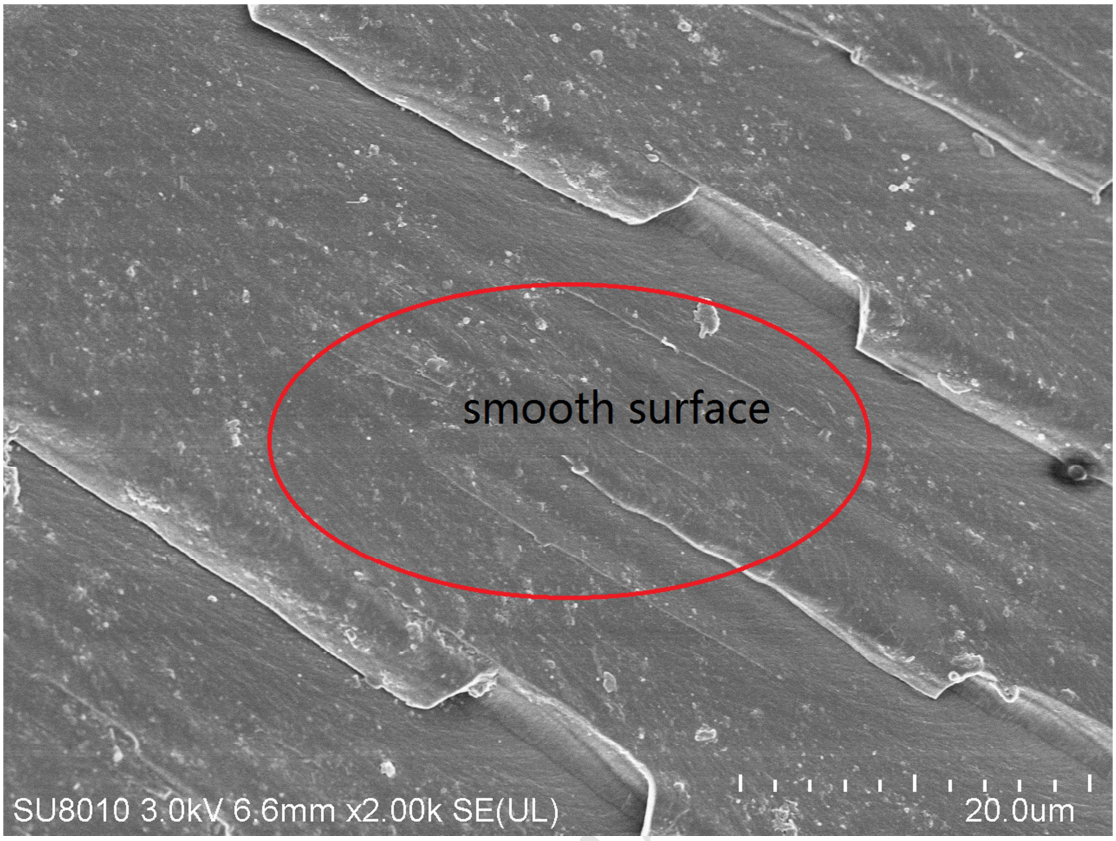

Figure 3a SEM image of the impact fracture surface of unmodified thermosets

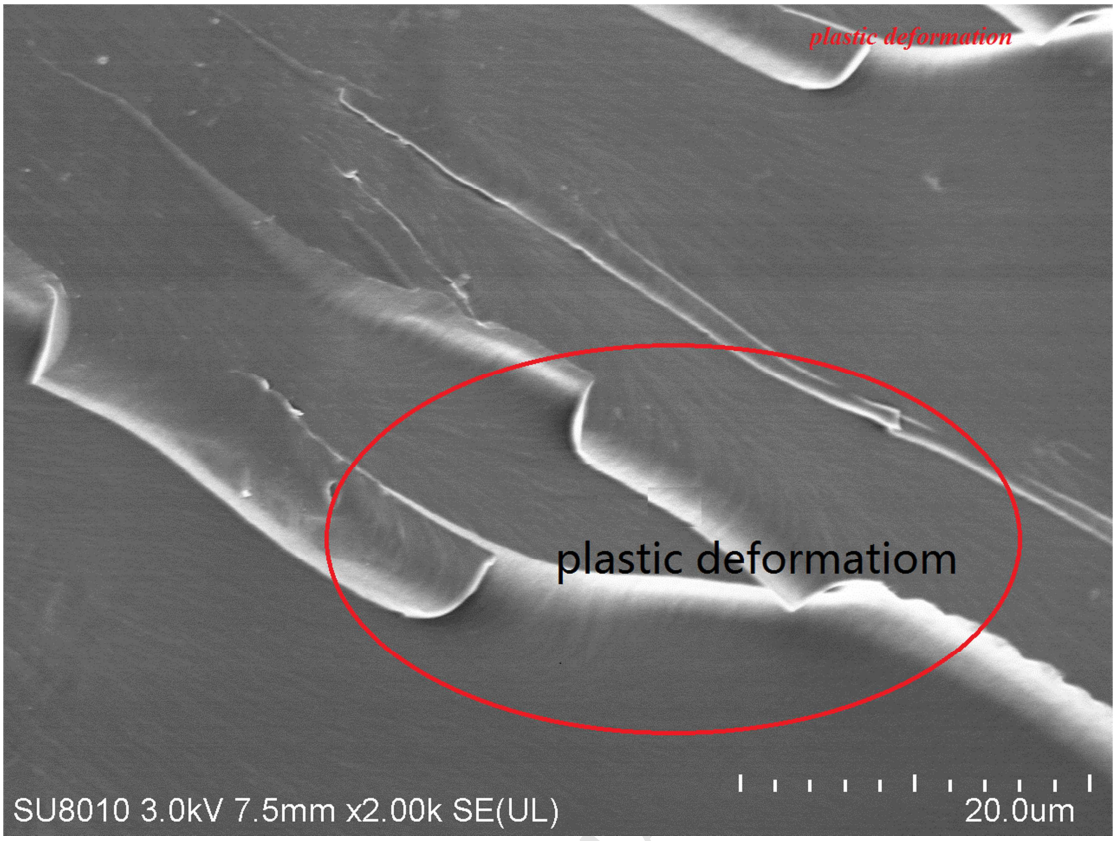

Figure 3b SEM image of the impact fracture surface of the 20 wt% HBPs modified thermosets

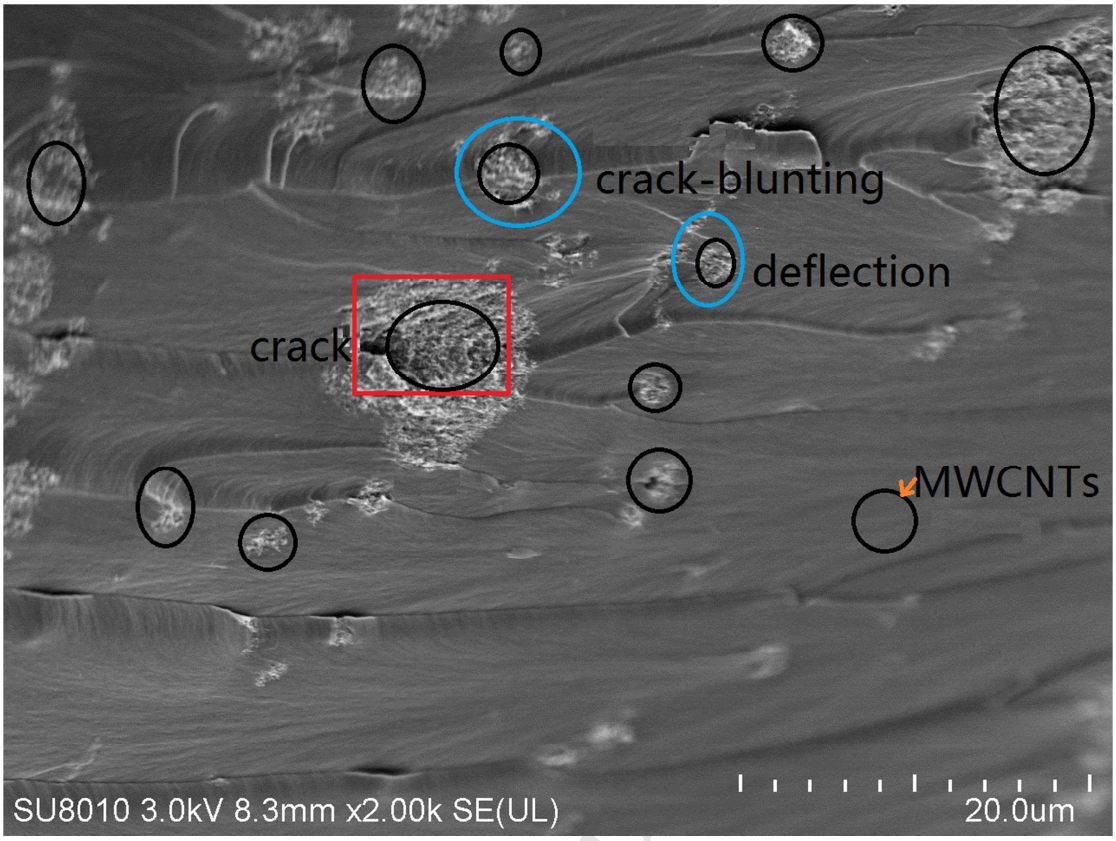

Figure 3c SEM image of the impact fracture surface of composites with 1.0 wt% MWCNTs

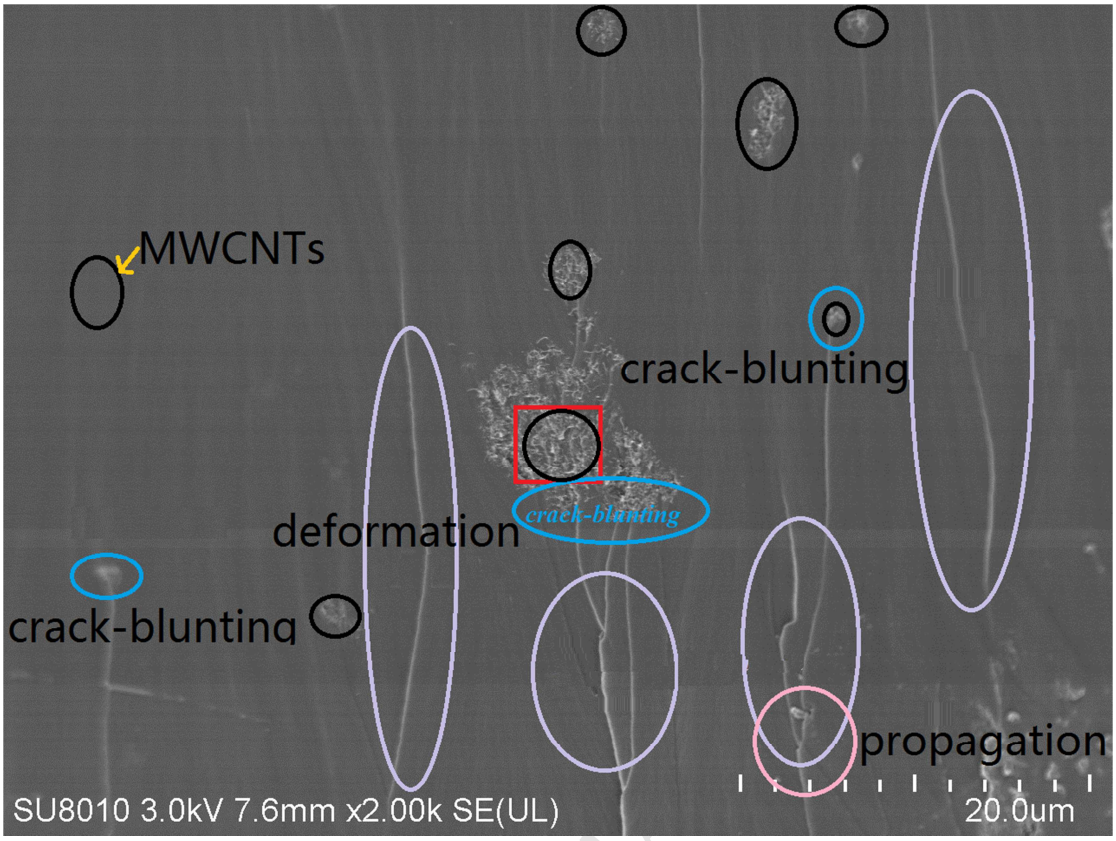

Figure 3d SEM image the impact fracture surface of composites with 20 wt% HBPs and 1 wt% MWCNTs

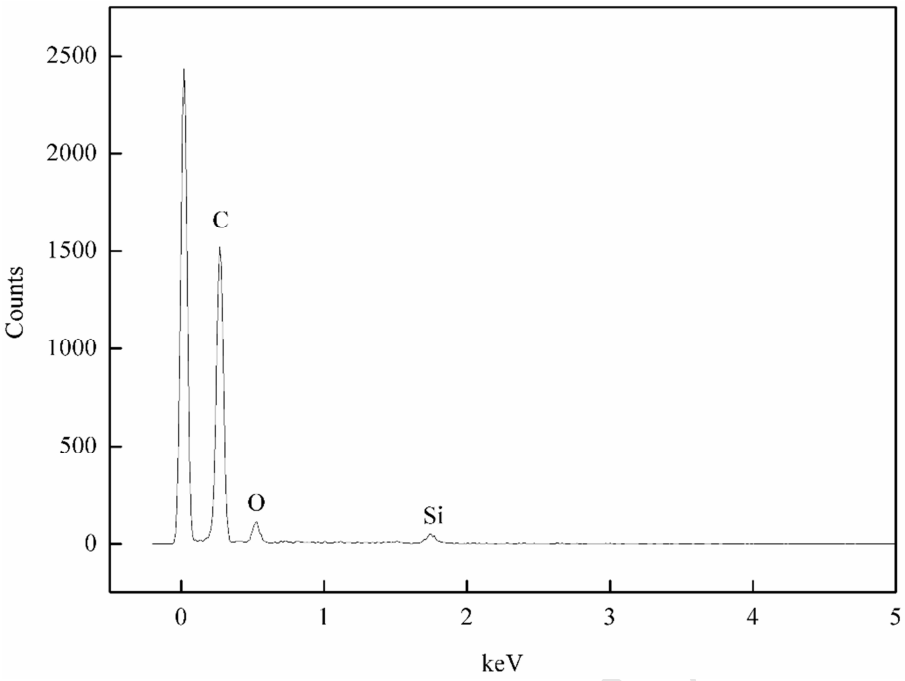

Figure 3e EDS spectrum of the selected area in Figure 3d (marked in red)

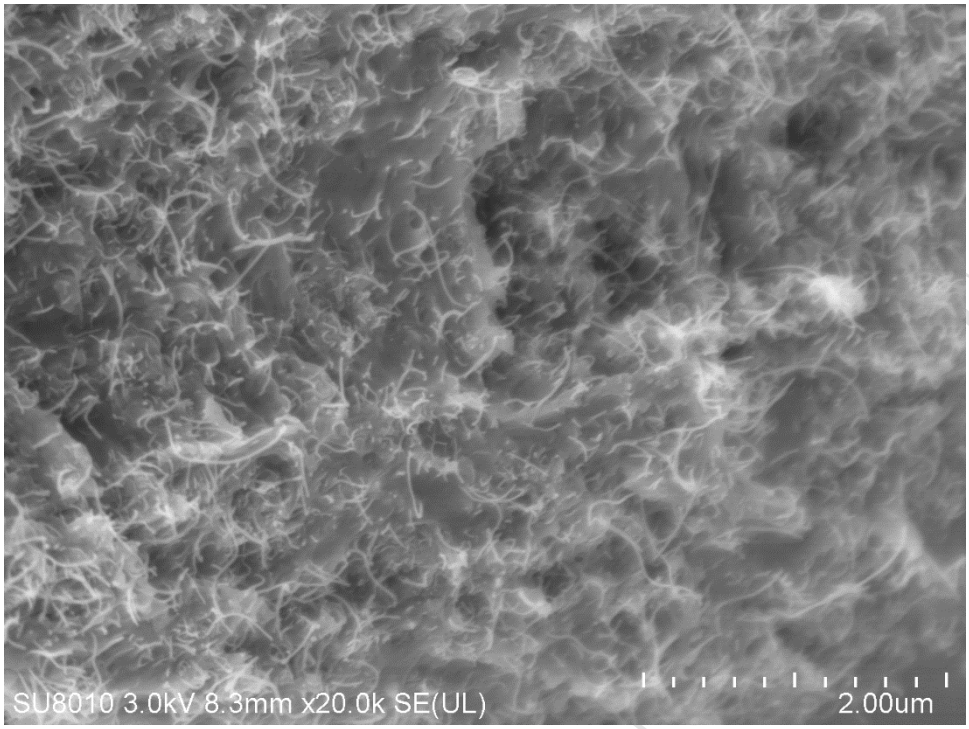

Figure 4a Magnified image of MWCNTs in composites with 1.0 wt% MWCNTs

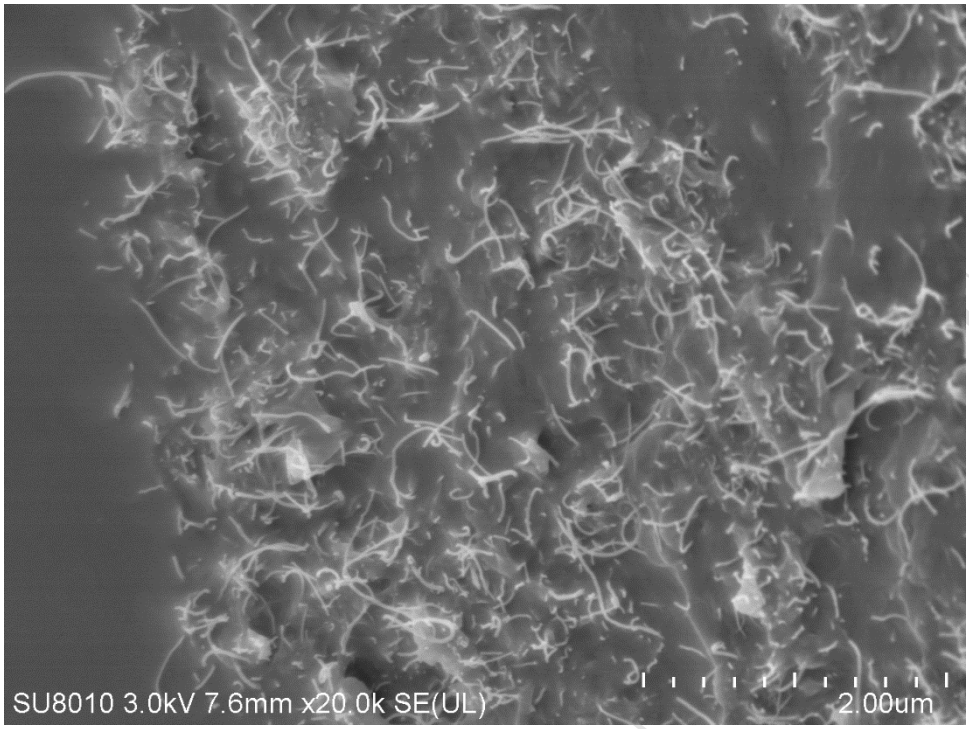

Figure 4b Magnified image of MWCNTs in composites with 20 wt% HBPs and 1 wt% MWCNTs